Random Access Preamble Design and Detection for 3GPP Narrowband IoT Systems

Xingqin Lin, Ansuman Adhikary, and Y.-P. Eric Wang

***Abstract*—Narrowband Internet of Things (NB-IoT) is an emerging cellular technology that will provide improved coverage for massive number of low-throughput low-cost devices with low device power consumption in delay-tolerant applications. A new single tone signal with frequency hopping has been designed for NB-IoT physical random access channel (NPRACH). In this letter, we describe this new NPRACH design and explain in detail the design rationale. We further propose possible receiver algorithms for NPRACH detection and time-of-arrival estimation. Simulation results on NPRACH performance including detection rate, false alarm rate, and time-of-arrival estimation accuracy are presented to shed light on the overall potential of NB-IoT systems.**

***Index Terms*—Random access, narrowband Internet of Things, machine-to-machine, machine type communications, low power wide area access.**

I. Introduction

INTERNET of Things (IoT) is a vision for the future world where everything that can benefit from a connection will be connected. Cellular technologies are being developed or evolved to play an indispensable role in the IoT world [1]. Narrowband IoT (NB-IoT), being developed in the 3rd generation partnership project (3GPP), promises to provide improved coverage for massive number of low-throughput low-cost devices with low device power consumption in delay-tolerant applications [2]. Prospective applications include utility metering, environment monitoring, asset tracking, and municipal light and waste management.

NB-IoT is based on orthogonal frequency-division multiple access (OFDMA) with 180 kHz system bandwidth. In this letter, we focus on NB-IoT physical random access channel (PRACH), known as NPRACH. NPRACH refers to the time-frequency resource on which random access preambles are transmitted. Transmitting a random access preamble is the first step of random access procedure that enables a user equipment (UE) to establish a connection with the network. Acquiring uplink timing is another main objective of random access in OFDMA systems. The acquired uplink timing is used to command the UE to perform timing advance to achieve uplink synchronization in OFDMA systems [3].

In Long Term Evolution (LTE), a set of random access preambles based on Zadoff-Chu (ZC) sequences is configured within a cell [3]. Existing works (see [4]–[6] and references therein) on random access for machine-to-machine (M2M) or IoT applications are centered on this ZC based PRACH design. We have proposed a new single tone PRACH design for NB-IoT [7]–[10]. The new PRACH design helps fulfill the important performance objectives of IoT such as long battery lifetime and extended coverage. Due to its advantages (described in Section II), the design has been accepted by 3GPP and is now an integral part of the international standard of NB-IoT [3]. The design and its rationale, however, may not be immediately clear to researchers not involved in the standardization process. Motivated by this, in this letter, we describe this new NPRACH design, share the design rationale, and discuss possible receiver algorithms for NPRACH detection. It should be stressed that this letter is not meant to be exhaustive but is intended as an accessible first reference for researchers interested in learning this new single tone random access channel design and potentially carrying out future research work in this area.

II. Random Access Preamble Design

3GPP has completed standardizing NPRACH design in Release 13 [3]. In this section, we first take a step back and describe the NPRACH design [7]–[10] in a more general way to facilitate understanding its design rationale. Then we use the standardized parameters to concretely illustrate the design.

Consider an OFDMA system with W Hz bandwidth and B Hz subcarrier spacing. The fast Fourier transform (FFT) size, denoted as N, is usually chosen as a power of 2 larger than the number W/B of subcarriers. The random access preamble design is based on single tone transmission with frequency hopping within a configured NPRACH band, as illustrated in Figure 1.

A classical OFDM symbol structure consists of a cyclic prefix (CP) portion and a data symbol. In order to maintain the orthogonality of the random access transmissions on different subcarriers, the CP has to be long enough to accommodate the initial uplink timing uncertainty in the cell that can be as large as the maximum round-trip delay (plus additional channel delay spread and downlink synchronization errors). Cellular IoT/M2M systems normally target at large cell deployment. For example, 35 km cell size should be supported for NB-IoT [11], requiring a CP at least as long as 233.3 μs. To reduce the relative CP overhead, we can repeat each N-sample OFDM symbol ξ times, and then add a single CP of N_{cp} samples. As a result, the length of the composite symbol is $N_{cp} + \xi N$ samples. The larger the number ξ of repetitions, the smaller the

Manuscript received August 10, 2016; accepted September 11, 2016. Date of publication September 15, 2016; date of current version December 15, 2016. The associate editor coordinating the review of this paper and approving it for publication was L. Le.

The authors are with Ericsson Research, San Jose, CA 95134 USA (e-mail: xingqin.lin@ericsson.com; ansuman.adhikary@ericsson.com; eric.yp.wang@ericsson.com).

Digital Object Identifier 10.1109/LWC.2016.2609914

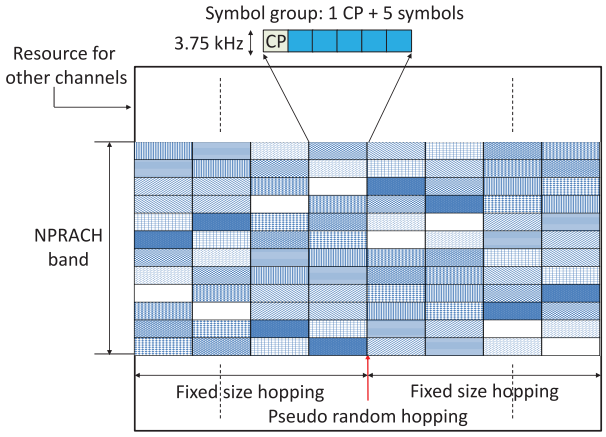

Fig. 1. Illustration of single tone NPRACH signal with frequency hopping: symbol groups of the same filled pattern belong to the same preamble.

CP overhead. The value of ξ however should be kept small enough such that the effect of channel variation is negligible within $N_{cp} + \xi N$ samples. Otherwise, undesirable inter-carrier interference (ICI) would arise. To avoid confusion with the classical notion of OFDM symbol, we refer to the composite symbol composed of $N_{cp} + \xi N$ samples as a *symbol group*. A random access preamble consists of L symbol groups and uses one subcarrier at every symbol group for transmission. The length L of the preamble is determined by the target operating signal-to-noise ratio (SNR) or equivalently, the target maximum coupling loss (MCL) in the networks.

To facilitate uplink timing estimation at base station (BS), the single tone preamble can hop across different subcarriers. Denote the subcarrier index used by symbol group m as $\Omega(m), m = 0, \ldots, L-1$, where $\Omega(\cdot)$ is a mapping from symbol group index to the subcarrier index. The mapping $\Omega(\cdot)$ characterizes the hopping pattern.

Standardized design parameters and hopping pattern: In the standard [3], NPRACH subcarrier spacing B is 3.75 kHz. Two CP lengths, 266.7 μs and 66.7 μs, are specified. The number ξ of symbols in a symbol group is specified to be 5. The standard treats 4 symbol groups as a basic unit. The basic unit can be repeated $2^j, j = 0, \ldots, 7$, times for coverage extension. Accordingly, the length L of a preamble equals $4 \times 2^j, j = 0, \ldots, 7$, symbol groups. Every preamble sequence takes a constant value "1", i.e., $u[m] = 1, m = 0, \ldots, L-1$, where $u[m]$ denotes the symbol value in symbol group m.

The hopping pattern of NPRACH illustrated in Figure 1 consists of both inner layer fixed size hopping and outer layer pseudo-random hopping. Outer layer pseudo-random hopping is applied between groups of 4 symbol groups. Inner layer fixed size hopping is applied within every 4 symbol groups. In particular, a single-subcarrier hopping is used between the first and the second and between the third and the fourth symbol groups, while a six-subcarrier hopping is used between the second and the third symbol groups.

In an OFDM resource grid with 180 kHz bandwidth, a cell can configure an NPRACH band consisting of 12, 24, 36, or 48 subcarriers for each coverage class. Accordingly, there are 12, 24, 36, or 48 orthogonal preambles, each being uniquely identified by its hopping signature. For contention based random access, a UE randomly selects one preamble to transmit. It is possible that multiple UEs may select the same preamble, resulting in a collision that can be resolved later in the random access procedure.

LTE PRACH vs. NB-IoT NPRACH: LTE PRACH is a multi-tone waveform with 1.25 kHz subcarrier spacing [3]. The modulated symbols in the frequency domain are based on ZC sequences of length 839, and thus the waveform occupies 1.05 MHz bandwidth that exceeds 180 kHz system bandwidth of NB-IoT. Further, though ZC sequences are constant-envelope, the PRACH signal after upsampling and filtering has a peak-to-average power ratio (PAPR) in the range of 2 to 7 dBs [8]. Non-zero PAPR induces power amplifier (PA) backoff, which in turn reduces coverage. PA backoff also gives rise to degraded PA efficiency, and thus has a negative impact on device battery life time. In contrast, NPRACH is a single-tone waveform that has close to zero PAPR. This low PAPR property is important to help NB-IoT achieve extended coverage and long battery lifetime of low cost IoT devices.

III. Rationale of Hopping Design Explained

A. Preliminary Analysis

To understand the rationale of NPRACH hopping, we carry out some analysis in this section. We start with $\xi = 1$ and extend the results to general ξ later. The baseband equivalent digital domain signal for the random access preamble transmission can be written as

$$s[n; m] = \frac{\sqrt{E}}{N} \sum_k S[k; m] e^{j2\pi \frac{k}{N} n}, n = -N_{cp}, \ldots, N-1,$$

where $s[n; m]$ denotes the n-th time domain sample of the m-th symbol group, E denotes the transmit energy per sample, and $S[k; m]$ denotes the symbol on the k-th subcarrier during the m-th symbol group. The narrow random access channel can be modeled as a one-tap channel. Denoting the channel coefficient at the n-th time domain sample of the m-th symbol group as $h[n; m] = a[m]$, where $a[m]$ is the channel gain at the m-th symbol group. The implicit assumption in the channel model is that the channel is invariant within one symbol group.

Denote by D the round-trip delay, i.e., time-of-arrival (ToA), to be estimated by the BS. By design, the CP is long enough such that $D \in [0, N_{cp} - 1]$. Accordingly, the n-th sample of the m-th symbol group at the receiver is given by

$$y[n; m] = a[m] \frac{\sqrt{E}}{N} e^{j2\pi \Delta f (n - D + m(N_{cp} + N))} \times \sum_k S[k; m] e^{j2\pi \frac{k}{N}(n-D)} + v[n; m], \quad (1)$$

where Δf is the residual carrier frequency offset (CFO) normalized by the sampling rate NB, and $v[n; m]$ is complex additive white Gaussian noise (AWGN) with zero mean and variance N_0. The residual CFO may be due to imperfect carrier frequency estimation during downlink cell search.

For each symbol group with $\xi = 1$, the receiver discards the first N_{cp} samples and performs a FFT on the remaining N samples. For $\xi > 1$, the receiver receives ξ symbols for every symbol group and performs ξ FFTs. The receiver then collects all the symbols received from the hopped subcarriers. The i-th received symbol in symbol group m can be written as

$$\tilde{y}[i;m] = B(\Delta f, D)a[m]u[m]e^{j2\pi\,\Delta f\left(m(N_{cp}+\xi N)+iN\right)} \times e^{-j2\pi\frac{\Omega(m)}{N}D} + \tilde{v}[i;m]. \quad (2)$$

where $\tilde{v}[i;m]$ denotes the noise and

$$B(\Delta f, D) = \sqrt{E}\frac{\sin(N\pi\,\Delta f)}{N\sin(\pi\,\Delta f)}e^{j2\pi\,\Delta f(\frac{N-1}{2}-D)}. \quad (3)$$

B. Design Rationale of NPRACH Frequency Hopping

Now we are in a position to discuss the rationale behind NPRACH hopping pattern, which is illustrated in Figure 1. From (2), it can be seen that the effect of ToA D is captured in the term $e^{-j2\pi\frac{\Omega(m)}{N}D}$. With hopping (i.e., varying $\Omega(m)$) the phases vary across symbol groups. Therefore, the BS can estimate ToA by processing the phases of the received symbols. Since the phase difference of two adjacent received symbol groups m and $m+1$ due to hopping is proportional to the hopping distance $|\Omega(m+1) - \Omega(m)|$, choosing a larger hopping distance provides a finer resolution for ToA estimate and thus better estimation accuracy. However, the phase difference is prone to 2π phase ambiguity, which may cause ambiguity in the ToA estimation. To avoid the 2π phase ambiguity, a larger hopping step $|\Omega(m+1) - \Omega(m)|$ reduces the ToA estimation range, which in turn translates into smaller cell sizes that can be supported.

There is a design tradeoff between ToA estimation range and accuracy when choosing a frequency hopping step size. This issue can be resolved with a multi-level frequency hopping pattern that includes both small and large hopping sizes. In NPRACH, singe-subcarrier hopping ensures large enough ToA estimation range for NB-IoT targeted cell sizes (up to 35 km). Six-subcarrier and pseudo random hopping improve ToA estimation accuracy. Pseudo random hopping brings in additional system level benefits including reduced inter- and intra-cell interference, reduced vain responses to preamble transmissions in neighboring cells, etc. With the multi-level frequency hopping, NPRACH design supports large ToA estimation range (which is needed for large cell size) while enabling acceptable ToA estimation accuracy at the BS.

IV. Receiver Algorithms

Based on the results and discussions in Section III, we now discuss how the BS can detect the random access preamble and estimate the ToA. We assume that $\{a[m]\}_{m=0}^{L-1}$ do not change in a block of Q symbol groups but change independently over the blocks. Note that this is not a requirement on the system but an assumption in the algorithm used by the BS. We choose Q such that the number L/Q of blocks is an integer. For example, $Q = 4$ is a reasonable value for NB-IoT since the standard treats 4 symbol groups as the basic NPRACH repetition unit [3]. The ToA and residual CFO can then be jointly estimated as follows.

$$(D^\star, \Delta f^\star) = \arg\max_{D,\Delta f} J(D, \Delta f) = \arg\max_{D,\Delta f} \sum_{g=0}^{L/Q-1} \left| J_g(D, \Delta f)\right|^2. \quad (4)$$

Here $J_g(D, \Delta f)$ equals

$$\sum_{m=gQ}^{(g+1)Q-1}\sum_{i=0}^{\xi-1} z[i;m]e^{-j2\pi\,\Delta f\left(m(N_{cp}+\xi N)+iN\right)}e^{j2\pi\frac{\Omega(m)}{N}D}, \quad (5)$$

where $z[i;m] = \tilde{y}[i;m]u^*[m]$.

The above rule (4) of joint ToA and residual CFO estimation is intuitive. The estimate $(D^\star, \Delta f^\star)$ is the one that yields the maximum correlation of the transmitted preamble symbols and the received symbols whose phase shifts due to ToA and residual CFO are corrected by the estimate. Note that the estimation rule (4) takes the form of a two-dimensional (2-D) discrete-time Fourier transform that can be implemented by a 2-D FFT. We take the long CP with $N_{cp} = N$ in NB-IoT as an example. Denote by M_1, M_2 the FFT lengths of the 2-D FFT. For each block of symbols, compute a 2-D FFT:

$$W_g[p,q] = \sum_{n=0}^{M_1-1}\sum_{k=0}^{M_2-1} w_g[n,k]e^{-j2\pi\frac{n}{M_1}p}e^{-j2\pi\frac{k}{M_2}q}, \quad (6)$$

where $w_g[n,k]$ is an $M_1 \times M_2$ array given by

$$w_g[n,k] = \begin{cases} z[i;m] & \text{if } n = (m-gQ)(\xi+1)+i,\ \ k = \Omega(m); \\ 0 & \text{otherwise.}\end{cases}$$

Summing the magnitude squares of the L/Q 2-D FFTs yields $\tilde{J}[p,q] = \sum_{g=0}^{L/Q-1}|W_g[p,q]|^2$. Let $(p^\star, q^\star)$ be the indices of the maximum value of $\tilde{J}[p,q]$. Then the residual CFO and ToA can be estimated as follows.

$$\Delta f^\star = \begin{cases} \frac{1}{NM_1}p^\star & \text{if } p^\star < \frac{M_1}{2}; \\ \frac{1}{NM_1}(p^\star - M_1) & \text{otherwise.}\end{cases}$$

$$D^\star = \begin{cases} -\frac{N}{M_2}q^\star & \text{if } q^\star < \frac{M_2}{2}; \\ -\frac{N}{M_2}(q^\star - M_2) & \text{otherwise.}\end{cases}$$

Assuming a joint estimate $(D^\star, \Delta f^\star)$ has been obtained, we can compare the statistic $J(D^\star, \Delta f^\star)$ to a predetermined threshold to determine the presence of the preamble. In particular, if the statistic exceeds the threshold, the BS declares the presence of the preamble; otherwise, the BS declares that the preamble is not present. *Misdetection* occurs if $J(D^\star, \Delta f^\star)$ does not exceed the detection threshold when the random access preamble is present. *False alarm* occurs if $J(D^\star, \Delta f^\star)$ exceeds the detection threshold when the random access preamble is absent.

V. Simulation Results

In this section, we provide some simulation results to evaluate the performance of NPRACH design. The simulation assumptions used are based on the ones outlined in [11], and are summarized in Table I. We consider three coverage classes

TABLE I
SIMULATION PARAMETERS

CP length	266.7 μs
Subcarrier spacing	3.75 kHz
Symbol group	1 CP and 5 symbols
NPRACH band	12 subcarriers
Channel model	Typical urban
Doppler spread	1 Hz
Antenna configuration	1 Tx; 2 Rx
Timing uncertainty	Randomly chosen between 0 and CP
Frequency error	Uniformly drawn from $\{-50, 50\}$ Hz
Frequency drift	Uniformly drawn from $\{-22.5, 22.5\}$ Hz/s
No. of iterations	10,000 for detection; 100,000 for false alarm

TABLE II
MISDETECTION AND FALSE ALARM PROBABILITIES

	Coverage 1	Coverage 2	Coverage 3
Target SNR	14.25 dB	4.25 dB	-5.75 dB
No. of symbol groups	8	32	128
Misdetection	29/10,000	24/10,000	84/10,000
False alarm	0/100,000	0/100,000	13/100,000

and configure 8, 32, and 128 symbol groups for the three coverage classes, respectively. The target operating SNRs for the three coverage classes are 14.25 dB, 4.25 dB and -5.75 dB respectively. Note that according to the evaluation setup agreed in [11], these three operating SNRs correspond to 144 dB MCL (nominal coverage of GSM/GPRS systems), 154 dB MCL and 164 dB MCL respectively.

The link level simulation process goes as follows.[1]

1) The transmitter randomly selects a preamble in the configured NPRACH band and maps the preamble symbols onto the OFDM resource grid.
2) The transmitter performs inverse FFT to obtain time domain samples and inserts CP accordingly.
3) The transmitter generates random access signal by up-sampling and filtering the time domain samples.
4) Pass the random access signal through a radio channel.
5) Add white Gaussian noise to the output of the channel.
6) The receiver filters and down-samples the received signal.
7) For each received symbol group in a preamble, the receiver discards the CP samples and performs FFTs on the remaining samples.
8) The receiver performs joint ToA and residual CFO estimation, and uses a threshold based approach to determine the presence of the preamble.

For false alarm testing, the input to the receiver is a Gaussian noise signal, therefore, the above Steps 1) – 4) are not needed.

Table II summarizes the misdetection and false alarm probabilities of the NPRACH design under the configured three coverage classes. It can be seen that the detection probabilities exceed 99%, while the false alarm probabilities are well below 0.1%. Figure 2 shows the distributions of ToA estimation errors for the three configured coverage classes. It can be seen that the ToA errors are within [-3, 3] μs with very high confidence level for all three cases. While NPRACH performance

[1]Steps 1) – 3) may be simplified by directly generating the single tone random access signal in time domain.

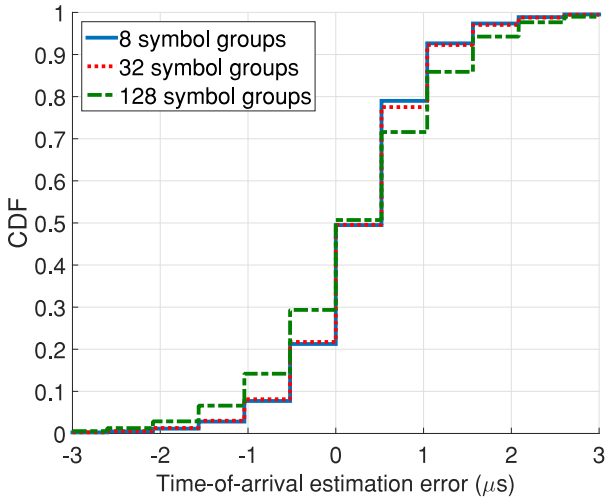

Fig. 2. Distributions of ToA estimation errors.

requirements are still under discussion in 3GPP, the results in this letter demonstrate the potential of NPRACH in fulfilling the extended coverage requirement and the achievable uplink synchronization accuracy.

VI. CONCLUSION

In this letter, we introduce the new single tone frequency hopping random access signal used by NPRACH in NB-IoT systems. We explain in detail the design rationale and propose some possible receiver algorithms for NPRACH detection and time-of-arrival estimation. We also present simulation results to shed light on NPRACH performance. Future work may consider developing more efficient and/or advanced receiver algorithms for NPRACH.

REFERENCES

[1] S. Andreev *et al.*, "Understanding the IoT connectivity landscape: A contemporary M2M radio technology roadmap," *IEEE Commun. Mag.*, vol. 53, no. 9, pp. 32–40, Sep. 2015.
[2] "Revised work item: Narrowband IoT (NB-IoT)," 3GPP, RP-152284, Dec. 2015.
[3] "Technical specification group radio access network; evolved universal terrestrial radio access (E-UTRA); physical channels and modulation; (Release 13)," 3GPP, TS 36.211 V13.2.0, Jul. 2016.
[4] A. Laya, L. Alonso, and J. Alonso-Zarate, "Is the random access channel of LTE and LTE-A suitable for M2M communications? A survey of alternatives," *IEEE Commun. Surveys Tuts.*, vol. 16, no. 1, pp. 4–16, 1st Quart., 2014.
[5] H. S. Jang, S. M. Kim, K. S. Ko, J. Cha, and D. K. Sung, "Spatial group based random access for M2M communications," *IEEE Commun. Lett.*, vol. 18, no. 6, pp. 961–964, Jun. 2014.
[6] C.-Y. Oh, D. Hwang, and T.-J. Lee, "Joint access control and resource allocation for concurrent and massive access of M2M devices," *IEEE Trans. Wireless Commun.*, vol. 14, no. 8, pp. 4182–4192, Aug. 2015.
[7] "Narrowband LTE—Random access design," R1-156011, 3GPP TSG-RAN1 #82bis, Ericsson, Stockholm, Sweden, Oct. 2015.
[8] "NB-IoT—Random access design," R1-157424, 3GPP TSG-RAN1 #83, Ericsson, Stockholm, Sweden, Nov. 2015.
[9] "NB-IoT—Design considerations for single tone frequency hopped NB-PRACH," R1-160093, 3GPP TSG-RAN1 AH-NB-IoT, Ericsson, Stockholm, Sweden, Jan. 2016.
[10] "NB-IoT—Singe tone frequency hopping NB-PRACH design," R1-160275, 3GPP TSG-RAN1 #84, Ericsson, Stockholm, Sweden, Feb. 2016.
[11] "Technical specification group GSM/EDGE radio access network; cellular system; support for ultra low complexity and low throughput Internet of Things; (Release 13)," 3GPP, TR 45.820, Aug. 2015.